STRUCTURE–PROPERTY RELATIONS IN NONFERROUS METALS

Alan M. Russell

Department of Materials Science and Engineering
Iowa State University

Kok Loong Lee

Corus Group

A JOHN WILEY & SONS, INC., PUBLICATION

STRUCTURE–PROPERTY RELATIONS IN NONFERROUS METALS

STRUCTURE–PROPERTY RELATIONS IN NONFERROUS METALS

Alan M. Russell

Department of Materials Science and Engineering
Iowa State University

Kok Loong Lee

Corus Group

A JOHN WILEY & SONS, INC., PUBLICATION

Published by John Wiley & Sons, Inc., Hoboken, New Jersey.
Published simultaneously in Canada.

Library of Congress Cataloging-in-Publication Data:

Russell, Alan M., 1950–
Structure–property relations in nonferrous metals / Alan M. Russell, Kok Loong Lee.
p. cm.
Includes bibliographical references and index.
ISBN-13 978-0-471-64952-6 (cloth)
ISBN-10 0-471-64952-X (cloth)
1. Nonferrous metals—Textbooks. I. Lee, Kok Loong, 1976–II. Title.

TA479.3.R84 2005
620.1′8—dc22 2004054807

Printed in the United States of America.

10 9 8 7 6 5 4 3 2 1

To Laurel, Jeffrey, Kristen, and Mark

CONTENTS

PART TWO

ADDITIONAL INFORMATION

References, Appendixes, Problem Sets, and Metal Production Figures are available at *ftp://ftp.wiley.com/public/sci_tech_med/nonferrous*

PREFACE

We have written this book as a textbook suitable for junior/senior-level undergraduate materials science students, but it is also intended to serve as a reference for practicing engineers. The book describes the relationships between the atomic structure, crystal structure, and microstructure of metals and their physical behavior (e.g., strength, ductility, electrical conductivity, corrosion, etc.). In Part One we present basic principles of the atomic and crystal structure, defects, and processing of metals. In Part Two we describe the properties and uses of all the metallic elements except iron. We are grateful for the reviews and helpful suggestions of Karl Gschneidner, Jr., L. Scott Chumbley, Alan Renken, Bruce Cook, Fran Laabs, Joel Harringa, and Timothy Ellis, who graciously contributed their time to improving both parts of the book.

The periodic table contains 83 metallic elements. We have observed that most metals texts focus primarily on iron, the dominant commercial metal. The 82 nonferrous metals are often lumped into one or two chapters and treated as "aluminum, copper, plus scattered comments about all those other metals." Many excellent books exist that are devoted entirely to one metal, but the reader seeking a broader, more comprehensive understanding of all nonferrous metals has heretofore found no single volume that addresses the entire spectrum of nonferrous metal properties and engineering applications. With this book we have striven to meet that need in a readily comprehensible format that emphasizes the needs of the engineer. References, appendixes, problem sets, and information about leading metal-producing nations and their annual production tonnages are available at *ftp://ftp.wiley.com/public/sci_tech_med/nonferrous*.

We have found that students learn most efficiently when specific, real-world examples can be given to support theory and general principles. The university climate biases authors to focus on graduate education, and the result is a wealth of "scholarly" books containing lengthy mathematical derivations and extended narratives on modeling. These books are inherently ill-suited to convey the excitement of engineering practice to undergraduate students. Even at their best, such books often do little to explain *why* the student should care about these fundamental principles. The result is that talented students may lose motivation and opt out of materials science for other careers. This book devotes a substantial portion of its content to examples of how the fundamental concepts and equations apply to real engineering practice. It shares with the reader the odd, surprising, and exciting ways that the structures of metals affect their behavior in modern engineering systems.

Two special features of the book are (1) short examples of the properties and uses of specific metals, and (2) features on structure–property relations that expand on a particular concept, explaining how it applies to the metal in question. These often describe little-known, unusual, or exotic features of the metallic elements, and it is our hope that they will maintain the interest of the student and motivate him or her to persevere through the sometimes arduous but unfailingly rewarding study of metals.

ALAN RUSSELL
K. L. LEE

April 2004

1 Crystal and Electronic Structure of Metals

To do exactly as your neighbors do is the only sensible rule.

—Emily Post, *Etiquette*, 1922

1.1 INTRODUCTION

One of the most remarkable qualities of metals is their precise, repeating atomic packing sequences. Periodic crystalline order is the equilibrium structure of all solid metals, and heroic measures in alloying or ultrarapid cooling (Sec. 7.3) are required to suppress it. Metals crystal structures are a dominant factor in determining their mechanical properties, and crystal structures play an important role in magnetic, electrical, and thermal properties as well. Thus, an understanding of the crystal structures of metals should precede any attempt to understand their properties.

1.2 CRYSTAL STRUCTURES OF THE METALLIC ELEMENTS

If atoms are assumed to behave as impenetrable solid spheres, many different atom-packing arrangements are geometrically possible. If the atoms in the model are permitted to deviate from hard spheres to assume ellipsoidal shapes that may encroach slightly on their neighboring atoms outer electron shells, the number of possible atom arrangements becomes infinite. Yet, despite the large number of possible crystal structures, more than 80% of all metallic elements (Fig. 1.1) have one of the four simple crystal structures shown in Fig. 1.2.

Three of the structures shown in Fig. 1.2 [all except body-centered cubic (BCC)] achieve the densest possible packing for equal-sized spheres (i.e., the volume inside the atom spheres occupies 74% of total crystal volume); and the BCC structure is nearly as efficient at filling space, with its 68% packing efficiency. When one considers the curve of bonding energy versus interatomic distance for two atoms (Fig. 1.3), it is clear that the bonding energy is greatest at interatomic spacings that correspond to atoms in the hard-sphere model touching each other. Note in Fig. 1.3 how the repulsive energy is essentially zero until the atoms are almost contiguous, then increases very steeply (typically about as r^{-8}!) as the outermost electron orbitals begin to overlap. These two factors combine to produce the greatest bonding energy when the atoms are closely packed; gaps between neighboring atoms are energetically disfavored. In addition, total metallic bonding energy is increased when each atom has the greatest possible number of nearest-neighbor atoms.

The hexagonal close-packed (HCP), face-centered cubic (FCC), and α-La hexagonal structures are nearly identical, differing only in the stacking sequence of their densest-packed planes

Structure–Property Relations in Nonferrous Metals, by Alan M. Russell and Kok Loong Lee

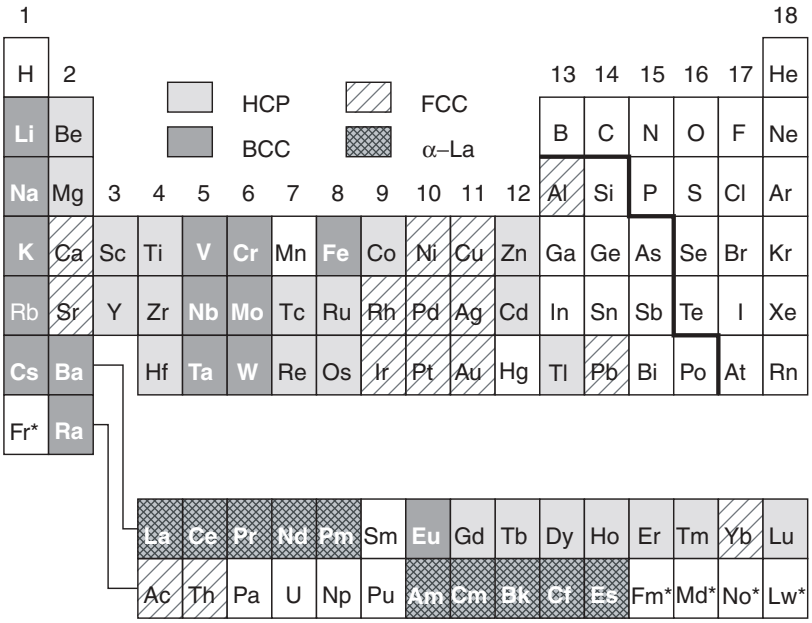

Fig. 1.1 Crystal structures of the metallic elements at 20°C and 1 atm pressure. (The asterisk denotes unknown crystal structure.)

(labeled A, B, and C in Fig. 1.2). Each atom in these three structures is surrounded by 12 nearest-neighbor atoms, the maximum number possible for equal-sized spheres. Since a BCC crystal is not a densest-packed structure, it might seem odd that it "outcompetes" the most densely packed structures to become the equilibrium structure of 15 metallic elements at room temperature. This is attributable to two effects. First, although each atom has only eight nearest neighbors in a BCC structure, the six second-nearest-neighbor atoms are closer in the BCC structure than in the FCC structure. Calculations indicate that BCC's second-nearest-neighbor bonds make a significant contribution to the total bonding energy of BCC metals. In addition, the greater entropy of the "looser" BCC structure gives it a stability advantage over the more tightly assembled FCC structure at high temperature. The BCC structure has unusually low resistance to vibration in the ⟨110⟩ direction, making lattice vibration in that mode especially easy. In the Gibbs free energy expression, ΔG is related to enthalpy (ΔH), absolute temperature (T), and entropy (ΔS) by

$$\Delta G = \Delta H - T\Delta S$$

The easier lattice vibration (greater ΔS factor) in BCC metals makes ΔG lower for BCC vis-à-vis FCC at higher temperatures. For this reason many metals have closest-packing structures at low temperature that transform to BCC at higher temperatures (Fig. 1.4). Half of all metallic elements possess one of the densest-packed structures at low temperature and transform to the slightly less densely packed BCC structure at higher temperature. The close-packed → BCC transformation usually occurs well above room temperature, but two of the low-melting alkali metals, Li and Na, are BCC at room temperature, with a transformation to a closest-packed structure (α-Sm, hR3, a variation of the α-La structure) at cryogenic temperatures.

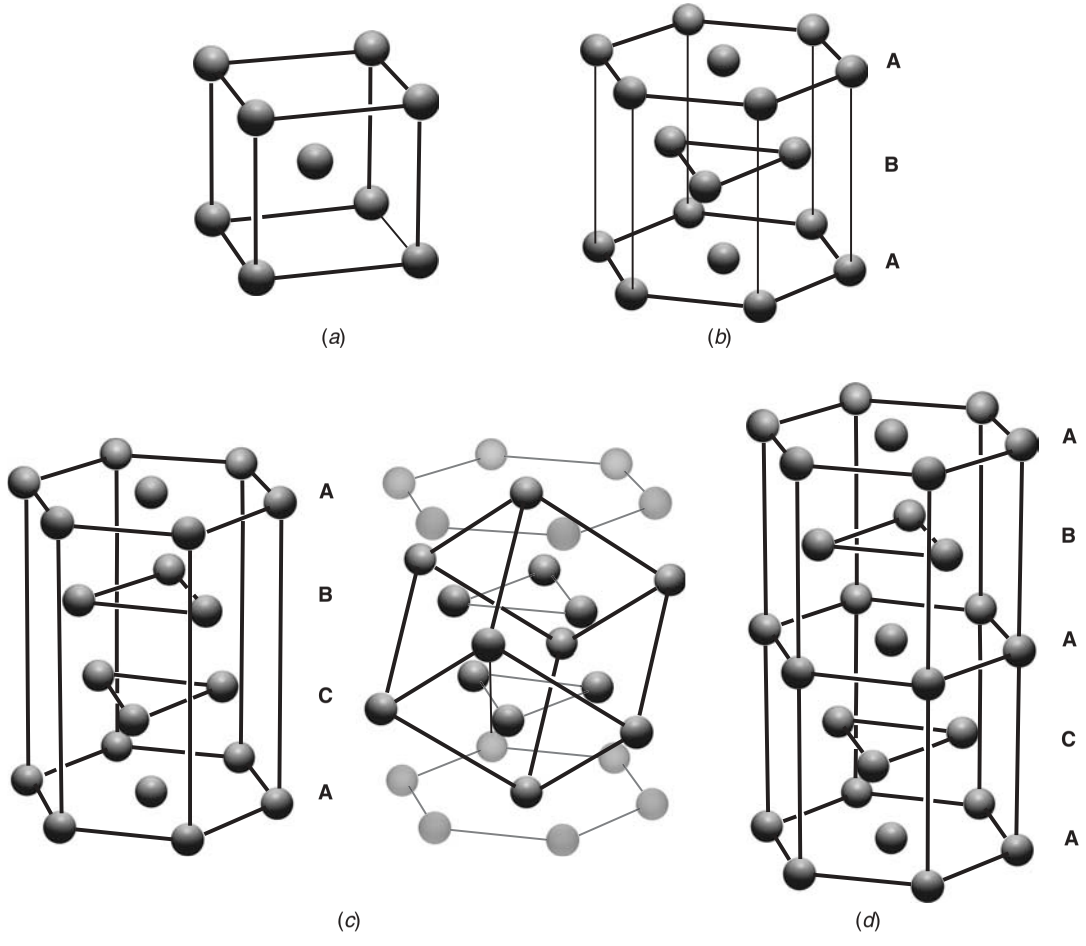

Fig. 1.2 Atomic packing sequences of (*a*) body-centered cubic; (*b*) hexagonal close-packed; (*c*) face-centered cubic (note that the face-centered cubic structure can be visualized in two seemingly different, but geometrically identical, depictions); (*d*) α-La hexagonal. Atoms are shown disproportionately small for clarity.

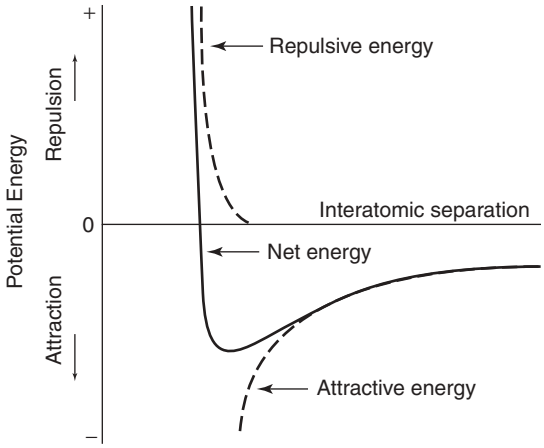

Fig. 1.3 Bonding energy versus interatomic spacing for two atoms. The solid curve is the sum of the attractive and repulsive energies. Although this plot represents the behavior of only two atoms, nearest-neighbor atoms in crystals behave similarly. The equilibrium interatomic spacing occurs at the minimum of the net bond energy curve.

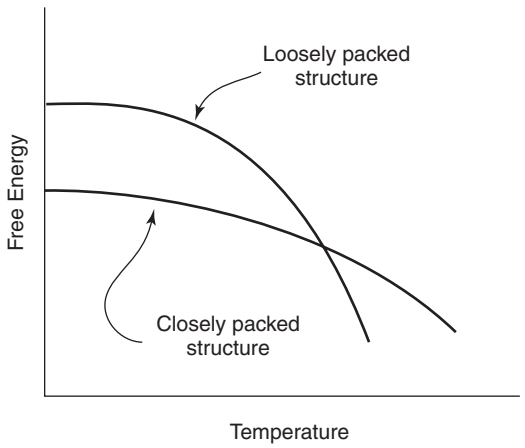

Fig. 1.4 Many metals transform from a closest-packed structure to a BCC structure at high temperature. The greater entropy (ΔS term) in the loosely packed BCC structure lowers ΔG more rapidly in BCC structures than in close-packed structures.

1.3 EXCEPTIONS TO THE RULE OF THE METALLIC BOND

Since stronger bonding occurs when metal atoms are in densely packed structures (HCP, FCC, α-La, or BCC), the key question is not why so few crystal structures predominate when so many are possible, but rather, why all metals don't crystallize in a closely packed structure? The answer to the latter question involves an intriguing shared bonding arrangement in some metals that is partially metallic and partially covalent.

Before embarking on a case-by-case narrative of metals that do not crystallize into HCP, FCC, α-La, or BCC structures, it is helpful to recall the nature of the metallic bond. Unlike ionic and covalent bonds, which have a specific electron exchange among a small number of atoms and a

certain directional character, the metallic bond is a delocalized release of the bonding electrons into the crystal. For this reason, metallic bonds are not strongly directional and can exist only when substantial numbers of atoms are present. For example, vaporized Au forms diatomic Au_2 molecules, but these molecules are covalent, not metallic. When many Au_2 molecules condense into a solid crystal, the bonding becomes metallic.

The 20% of metallic elements that possess less densely packed crystal structures at 20°C deviate from the norm because their bonding is partly covalent. As Fig. 1.1 shows, the metals in the lower left region of the periodic table all possess one of the densely packed crystal structures typical of nearly pure metallic bonding. However, covalent tendencies appear as one moves closer to the nonmetals on the periodic table. For example, Be lies next to the nonmetal B. Be is an HCP metal, but its *c*/*a* ratio is unusually low at 1.57 (1.633 is ideal for close-packed spheres). This distortion of the Be atom and the unusually high elastic modulus of Be (296 GPa) result from a covalent component in its bonding (Sec. 11.3). Contributions from covalency are also seen in Zn and Cd, which are both HCP metals with *c*/*a* ratios greater than 1.85. This lowers their packing density to about 65%, considerably less than the 74% of the ideal HCP structure (Sec. 19.2.2.2).

Of course, some metals do more than show distortions in a densely packed structure. As one moves rightward across the periodic table, progressively greater numbers of metals have "odd" structures (i.e., not HCP, FCC, BCC, or α-La). Most metals bordering the nonmetals possess more complex structures with lower packing density because covalent effects play a large role in determining their crystal structures; the directionality of covalent bonding dictates fewer nearest neighbors than exist in densely packed crystals.

Mn is the first odd crystal structure encountered as one moves left to right across the main section of the periodic table. All Mn's neighboring elements in the periodic table possess simple, conventional crystal structures, but Mn has extraordinarily complex structures. These are attributed to magnetic effects (Sec. 15.3.1). The room-temperature phase, α-Mn (cI58) (Sidebar 1.1) is stable below 727°C. From 727 to 1100°C, the equilibrium β-Mn structure is also quite complex (cP20). At higher temperatures, lattice vibrations nullify magnetic effects and Mn transforms to "normal" FCC and BCC phases.

Aside from Mn, all the remaining transition elements display normal metal crystal structures except Hg. Hg is a liquid at room temperature, but when it finally solidifies at −39°C, it forms a rhombohedral crystal (hR1) with 61% packing efficiency. Hg is weakly bonded because it is difficult to ionize the filled subshells of Hg (Xe core $+ 4f^{14}5d^{10}6s^2$). Hg's ionization energy (1007 kJ/mol) is the highest of all metals, and those of its congener elements Zn and Cd are only slightly lower. Since the *d* shells are filled completely in these group 12 metals, only *s* and *p* electrons are available for bonding, making them substantially weaker and lower melting than the neighboring group 11 elements. Zn and Cd hybridize to form $4s^1 + 4p^1$ and $5s^1 + 5p^1$ outer electron structures, which provide two electrons for bonding. Hg does this less well (Sec. 19.4.2.1), making Hg the lowest melting of all the metallic elements.

The lanthanide metals display a fascinating array of polymorphic phases below room temperature and at high pressure, but all lanthanides possess densely packed crystal structures at 20°C. The α-Sm structure is a stacking variation of the α-La structure, but it is a closest-packed structure. The room-temperature crystal structures of the actinide metals, however, are not as simple. Ac and Th are FCC, and the higher *Z*-number actinides (Am to Es) all have a densest-packed α-La structure at room temperature. However, the elements Pa through Pu have 5*f* electron participation in bonding, which produces low-symmetry structures at 20°C: tetragonal (tI2) Pa, orthorhombic U (oC4) and Np (oP8), and monoclinic Pu. Even in Pu's simpler high-temperature FCC structures (δ-Pu and δ′-Pu), the coefficient of thermal expansion is negative, a clear manifestation of a covalent component to the bonding (Sec. 24.5.3.1).

For metals near the nonmetals on the right side of the periodic table, electronegativities are high, covalency becomes a major part of the bonding, and dense-packed crystal structures are seen only in Al (FCC), Pb (FCC), and Tl (HCP). Ga (oC8) possesses a weakly bonded structure (Fig. 1.5) that provides each Ga atom with one nearest neighbor (0.244 nm away) and three

SIDEBAR 1.1: PEARSON SYMBOL NOTATION

In an effort to catalog the thousands of possible crystal structures observed in elements and compounds, crystallographers have developed the Pearson notation for crystal structures. This simple combination of two letters and a number provides a description of the structure according to the following precepts:

- The first letter (lowercase) identifies the crystal family:

  a = triclinic

  m = monoclinic

  o = orthorhombic

  t = tetragonal

  h = hexagonal, trigonal (rhombohedral)

  c = cubic

- The second letter (uppercase) identifies the Bravais lattice type:

  P = primitive

  I = body-centered*

  F = all cell faces contain a face-centered atom

  C = side or base faces are face-centered

  R = rhombohedral

- The number indicates the total number of atoms per unit cell.

Examples: Cu is a face-centered cubic metal; its Pearson notation is cF4 (cubic, Face-centered on all cell faces, 4 atoms per unit cell). Mg is a hexagonal close-packed metal; its Pearson notation is hP2 (hexagonal, Primitive, 2 atoms per unit cell).

Although the Pearson notation does not always define a unique crystal structure (e.g., somewhat different structures can all be mC2), it provides a concise description of the general nature of the crystal. Table 1.1 correlates the Pearson notation with the Bravais lattices.

* English speakers may wonder why the letter "I" is used for body-centered atoms rather than "B." The "I" stands for *innenzentrierte*, German for "produced from the inside center."

additional pairs of next-nearest neighbors that are 0.270, 0.273, and 0.279 nm away. This odd structure somewhat resembles covalently bonded Ga_2 "molecules" within a metal lattice. When Ga melts (30°C), it loses this unusual structure and contracts 3.4% (Sec. 20.3.2). In's structure is body-centered tetragonal (tI2), although its distortion from the BCC structure is small.

The lighter group 14 elements (Si and Ge) crystallize in the diamond structure (cF8). In their ground state (s^2p^2), these elements have only two p electrons in an unfilled subshell, but they hybridize to a s^1p^3 configuration that provides four electrons from partially filled subshells, all of which participate in forming covalent bonds with the four nearest-neighbor atoms (Fig. 1.6). The energy required (95 kcal/mol) to promote one electron from a Si atom's outer s subshell to the outer p subshell is more than offset by the stronger bonding afforded by four electrons rather

TABLE 1.1 Pearson Symbols for the 14 Bravais Lattices

Pearson Symbol	Bravais Lattice
aP	Triclinic
mP	Simple monoclinic
mC	Base-centered monoclinic
oP	Simple orthorhombic
oC	Base-centered orthorhombic
oF	Face-centered orthorhombic
oI	Body-centered orthorhombic
tP	Simple tetragonal
tI	Body-centered tetragonal
hP	Hexagonal
hR	Rhombohedral
cP	Simple cubic
cF	Face-centered cubic
cI	Body-centered cubic

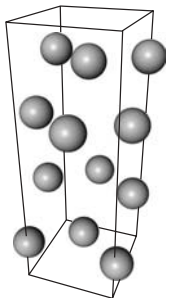

Fig. 1.5 oC8 structure of Ga. This layered structure provides one nearest neighbor for each atom and three pairs of next-nearest neighbors. Ga's packing efficiency is low (39%), and its density actually increases upon melting. Atoms are shown disproportionately small for clarity.

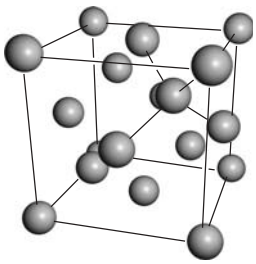

Fig. 1.6 cF8 diamond cubic structure of C (diamond), Si, Ge, and α-Sn. Covalent bonding predominates over metallic bonding in these tetravalent elements. Each atom has only four nearest neighbors, yielding a low packing efficiency (34%). The nearest neighbors of one atom are indicated by lines to the neighboring atoms. Atoms are shown disproportionately small for clarity.

than two. Si and Ge are classic metalloids, possessing a crystal structure determined by their predominantly covalent bonding but displaying somewhat metal-like optical and conductivity behavior (Sec. 21.2.2). At room temperature, β-Sn has a low density (53% packing efficiency) tI4 structure with $5s^2 5p^2$ electronic structure displaying both covalent and metallic bonding. At

13°C, β-Sn transforms to the even less densely packed α-Sn cF8 diamond cubic structure with $s^1 p^3$ hybridized covalent bonding.

The group 15 metals As, Sb, and Bi all share an hR2 structure that allows each trivalent atom to bond covalently with three nearest neighbors in a sort of "puckered layer" geometry. The interatomic spacing within an As layer is 0.252 nm, and the spacing between layers is 0.312 nm. These elements still retain metal-like electrical conductivity, although the crystal structure is clearly dictated by the covalent bonding component (Fig. 22.1). Finally, Po, the only group 16 element with predominantly metallic character, has a simple cubic (cP1) structure with six nearest neighbors for each atom and a packing efficiency of 52% (Sec. 22.5.2).

Physical properties important to the engineer are strongly influenced by crystal structure. Perhaps the most important property related to crystal structure is the metal's ductility (or lack thereof). Densely packed structures usually allow free dislocation motion on one or more slip planes, permitting the metal to deform plastically without fracturing. Ductility is vital for easy formability and for fracture toughness, two properties that give metals a great advantage over ceramic materials for many engineering uses. Metals with an HCP, FCC, BCC, or α-La crystal structure are usually ductile at room temperature; most metals with less densely packed structures have little or no ductility until they approach their melting temperatures.

1.4 EFFECTS OF HIGH PRESSURE ON CRYSTAL STRUCTURE

The electrons of a metal form a "band structure" of electron energies. As Fig. 1.7*a* shows, the half-filled 3*s* band in Na provides the electrons for the metallic bond. Only a tiny amount of extra energy is needed to promote electrons in the 3*s* band to higher, previously unoccupied energy levels in the band. This allows Na to carry electric current easily, and it contributes to thermal conductivity as well. In Mg the structure is somewhat different (Fig. 1.7*b*), but the resulting physical properties are similar; the filled 3*s* band overlaps the empty 3*p* band, and the energy needed to promote a 3*s* electron into the empty 3*p* band is negligibly small, conferring classic metallic behavior on Mg. For the transition metals Sc through Ni, a partially filled 3*d* band overlaps the 4*s* band. This provides fairly easy access for electron promotion to unoccupied states, although complex interactions between these two bands reduce conductivity somewhat. The exceptionally high electrical conductivity of group 11 metals (Cu, Ag, Au) results from a half-filled *s* outer subshell and the lack of interaction with the filled *d* band (Sec. 18.1). Similar behaviors occur in all the other metals of the periodic table, although elements near the

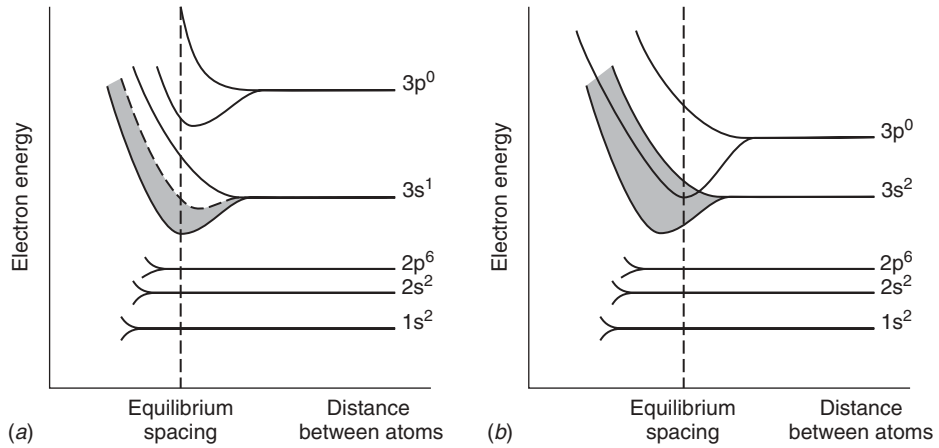

Fig. 1.7 Simplified electronic band structure depictions for crystals of (*a*) Na and (*b*) Mg.

nonmetals, such as Si and Ge, have a small gap between the filled lower-energy electron band and the empty higher-energy electron band. This sharply reduces electrical conductivity, because only a small fraction of the electrons can acquire enough energy from thermal excitation to jump the bandgap (Sec. 21.2.2). For most nonmetals, the bandgap is so large that thermal excitation cannot promote appreciable numbers of electrons; these materials lack mobile electrons and are electrical insulators.

Note in Fig. 1.7 that the 3*s* and 3*p* subshells form bands, but the noninteracting inner orbitals ($1s^2 2s^2 2p^6$) have discrete energy levels (rather than bands) at the equilibrium spacing between neighboring atoms. Of course, single atoms of Na and Mg vapor would have no bands; all the electron levels would be single values like the 1*s*, 2*s*, and 2*p* levels shown in Fig. 1.7. The Pauli exclusion principle requires that only two electrons may have the same energy in the crystal, so enormous numbers of extremely closely spaced but different energy levels exist, forming the energy bands.

In the Na case, the 3*s* band is only half full, so electrical conductivity is high. In the Mg case, conductivity is also high because the filled 3*s* band overlaps the empty 3*p* band. By applying pressure to a metal, the dashed vertical line marking the equilibrium spacing of atoms in Fig. 1.7*b* effectively moves leftward. This changes the overlaps and gaps between bands, altering the number and types of electrons available for bonding. Under high pressure, this effect can convert semiconducting metalloids into ordinary metals, and vice versa.

Si provides an example of how a metalloid element with lower packing density can be changed into simpler, more densely packed metallic structures at high pressure. At normal pressures, Si has predominantly covalent bonding, a coordination number of 4, and rather low electrical conductivity. However, increasing pressure drives Si through a series of transformations (Appendix A, *ftp://ftp.wiley.com/public/sci_tech_med/nonferrous*) that progressively increase the coordination number first to 6 (tI4), then 8 (hP1), and finally to 12 (cF4, FCC). The electrical conductivity increases by several orders of magnitude as pressure rises, and the final result is a "normal" FCC metal whose properties are much different from those of diamond cubic (cF8) Si. It should be noted that the pressures necessary to achieve these transformations are exceptionally high. One atmosphere is 0.1 MPa. Si's transformation to tI4 occurs at 12 GPa (120,000 atm), and the transformation to cF4 requires 78 GPa (780,000 atm). For comparison, the water pressure at the greatest ocean depth (>11,000 m) is "only" 0.1 GPa (1150 atm).

High pressure does not always cause transformation to simpler crystal structures. In some metals (e.g., Rb, Bi) pressures in the range 15 to 30 GPa actually convert comparatively simple crystal structures into phases with hundreds of atoms per unit cell. Intriguingly, some materials will retain nonequilibrium, high-pressure crystal structures after the applied pressure is removed. A familiar example of this behavior occurs in the commercial process of transforming graphite to diamond in high-pressure cells; the resulting diamond is metastable, but it persists indefinitely at ambient temperature and pressure. Research efforts in high-pressure materials science are producing many new materials, some of which survive the decompression from high pressure to ambient pressure, yielding ultrahard materials (e.g., cubic BN and c-BC_2N), optoelectronic semiconductors, and magnetic materials. The "workhorse" research apparatus for studying high-pressure phase transformations is the diamond-anvil cell, but most units can compress only milligrams of material. However, other technologies are capable of producing pressures almost as high as the diamond-anvil cell on quantities large enough to be technologically useful (in the range of cubic centimeters). High-pressure phases that can survive the decompression to ambient pressure promise to greatly expand the material choices available to design engineers in the decades to come (Sidebar 1.2).

1.5 EFFECT OF ELECTRONIC STRUCTURE ON CRYSTAL STRUCTURE

The *metallic bond* is often described as a gas or cloud of electrons adrift in the lattice of their parent ions. This simple description is useful in providing an easily visualized model consistent

SIDEBAR 1.2: METALLIC HYDROGEN AND JUPITER'S CORE

In 1935 theorists predicted that H would transform to a metal at ultrahigh pressures. Some calculations even suggest that once formed, metallic H might be metastable at 1 atm of pressure and that metallic H might be an electrical superconductor at room temperature. Unfortunately, until recently no laboratory system existed to test this prediction. The definitive test for transformation to a metallic state is a large increase in electrical conductivity, but diamond-anvil cells cannot test conductivity while applying such high pressures.

In 1996 a team of scientists at Lawrence Livermore Laboratory subjected liquid H to impact from a metal plate moving 7 km/s. During a 200-ns period after initial impact, the electrical conductivity of the H increased by a factor of 10^4 as the pressure in the H exceeded 140 GPa (1.4 million atm). This was the first direct evidence of successful metallization of H on Earth. Although the experiment was not designed to produce persistent samples of metallic H, it is the first step toward developing production processes. If metastable metallic H could be produced, it might be an excellent ultralightweight structural material. The engineering benefits of a room-temperature superconductor are obvious. If it is possible to trigger a sudden transformation of metallic H to normal H, a powerful explosive or potential rocket fuel might result.

Metallic hydrogen production remains a daunting materials engineering challenge. However, astronomers have strong evidence that the interiors of the massive gas planets Jupiter and Saturn are mostly metallic H (Fig. 1.8). Jupiter's intense magnetic field matches theoretical predictions of highly conductive H beneath the planet's outer atmosphere. Recent discoveries of large numbers of massive planets orbiting other stars suggest that metallic H planets may be quite common throughout the universe. If so, metallic H may be the most exotic terrestrial metal but the most common metal in the universe as a whole.

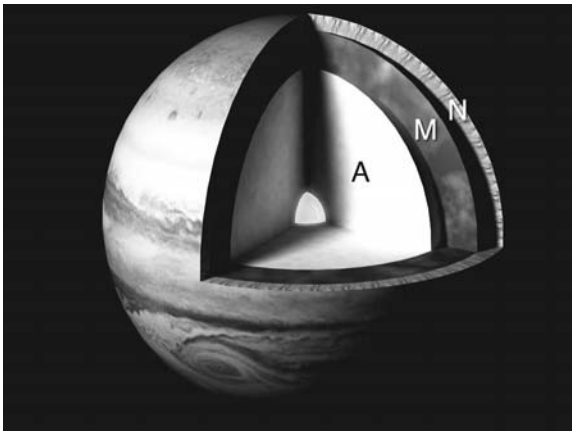

Fig. 1.8 Pictorial section view of the interior of Jupiter. Most of the planet is believed to be metallic H containing smaller amounts of other elements. The regions are labeled as N (normal molecular hydrogen), M (metallic molecular hydrogen), and A (metallic atomic hydrogen). Mixed rock and ice comprise the small central core.

with ordinary metals' high electrical conductivity and nondirectional bonding. However, it does not provide a quantitatively accurate description of metallic heat capacity and other physical properties. Throughout most of the twentieth century, physicists and materials scientists worked to refine the models of electron behavior in metals to describe their crystal structures and mechanical, electrical, and magnetic properties more accurately.

In principle it should be possible to use the Schrödinger equation from quantum mechanics to calculate the wave function of a free electron gas in a metallic crystal. This can be done if it is assumed that the electrons are not affected by the atoms in the metal lattice. Since the Pauli exclusion principle requires that no more than two electrons may have the same energy within the crystal, a population distribution of electrons occupying extremely closely spaced (but separate) energy levels results, as plotted in Fig. 1.9. The curve is a plot of the density-of-states function:

$$n(E) = \left(\frac{V}{2\pi^2}\right) E^{1/2}$$

where $n(E)$ is the density of states, V the crystal volume, and E the electron kinetic energy. At 0 K a sharp cutoff of occupied states occurs at the Fermi energy, E_F; above 0 K some electrons in states just below E_F will be thermally excited to occupy formerly empty states above E_F. This "rounds off" the sharp step at E_F, but at room temperature, the effect is rather small, and the overall appearance of the plot in Fig. 1.9 changes little.

The plot in Fig. 1.9 is based on the simplifying assumption that the ion cores of the atoms in the metal lattice do not affect the electron cloud. Not surprisingly, this assumption introduces error into the prediction of the electron behavior within a metal. Since the first Schrödinger equation calculations for Na metal (a particularly simple case) were published in 1933, a continuous progression of improvements and refinements in these computations has occurred. It is much more difficult to perform these computations for polyvalent metals and transition metals because multiple interactions must be accounted for, which greatly increases the complexity of the computation. Of course, most of the periodic table is comprised of polyvalent metals and transition metals. Indeed, this proved to be one of the great intellectual challenges of the twentieth century, and the process is still a work in progress. Even the best computations are still only estimates of electron behavior in metals, but the accuracy of the estimates has become quite impressive in recent years.

Figure 1.10 shows the result of density-of-states computations for two nontransition metals (i.e., all bonding electrons are s and p type, no d electrons). Al provides an example of a metal that conforms closely to the free-electron-model density of states in Fig. 1.9. By contrast, Be deviates sharply from that case and is nearly a semiconductor because its density-of-states plot approaches zero near the Fermi energy. A gap in the plot at E_F would greatly decrease electrical

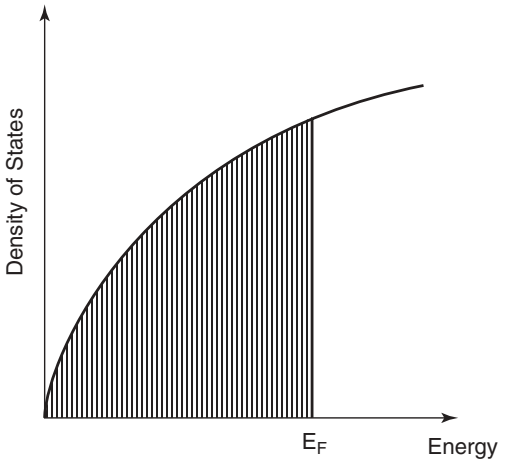

Fig. 1.9 Density of states (i.e., the energy distribution) of an idealized free electron cloud in a metal crystal at 0 K (solid line). E_F is the Fermi energy, the highest occupied electron energy level in the crystal at 0 K.

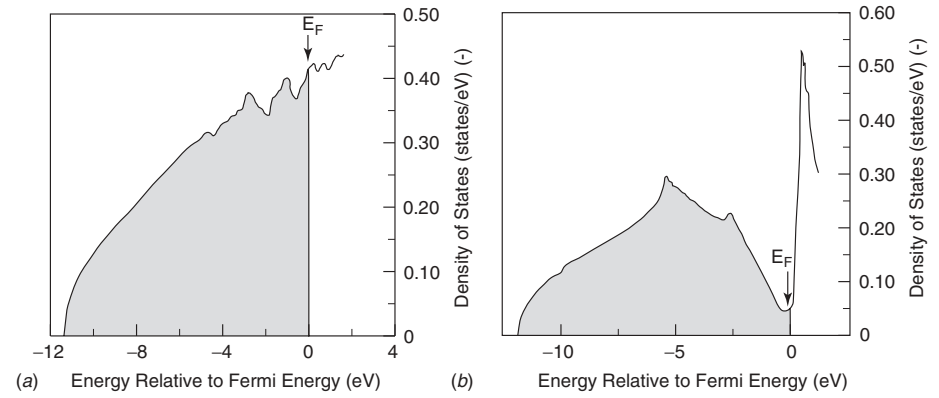

Fig. 1.10 (*a*) The density-of-states function calculated for Al closely matches the idealized nearly free electron model of Figure 1.9. (*b*) By contrast, calculations for Be show substantial deviation from the idealized DOS. Be nearly has a bandgap at E_F, which would make it a semiconductor. (Redrawn from Moruzzi et al., 1978, pp. 41 and 53.)

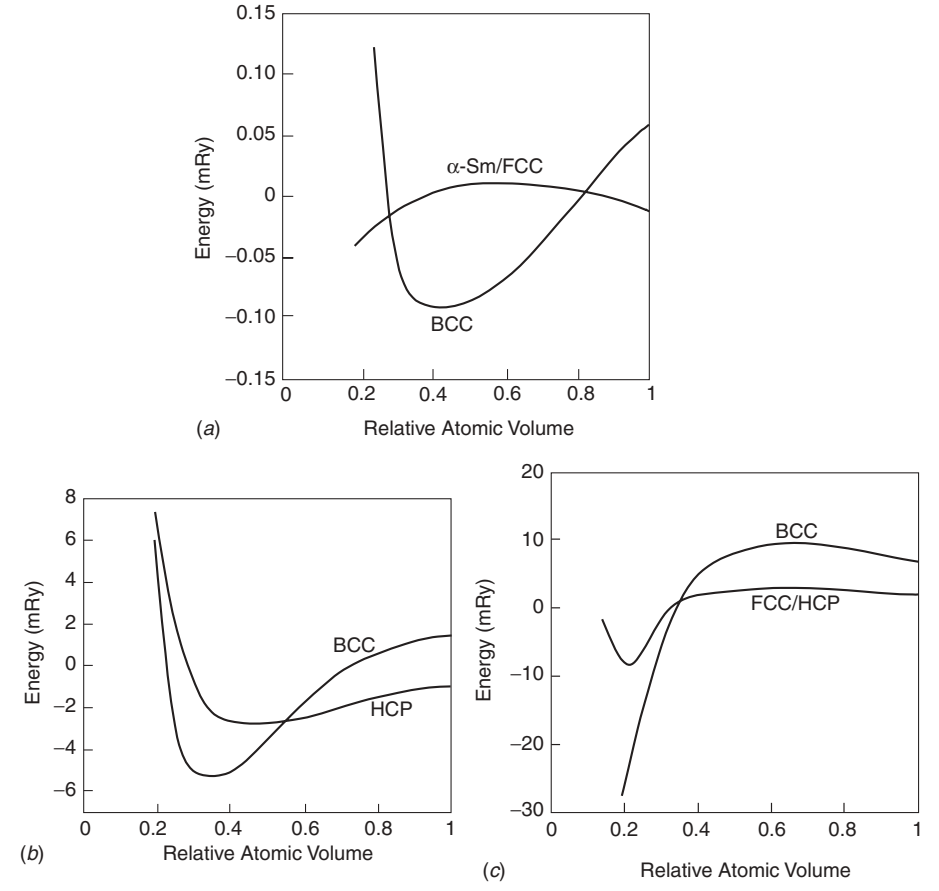

Fig. 1.11 Relative free energies at 0 K of various crystal structures calculated for (*a*) Na, (*b*) Mg, and (*c*) Al. Relative atomic volume (actual atomic volume/equilibrium atomic volume) is 1 at atmospheric pressure. The mRy is an energy unit equal to 0.0136 eV. (Redrawn from Moriarity and McMahon, 1982.)

conductivity, since thermal excitation would be required to promote electrons across the gap into empty states, where they could move in response to a voltage gradient in the crystal.

Calculations can also be made to predict crystal structure transformations in metals as a function of applied pressure. The results of such computations are shown in Fig. 1.11 for Na, Mg, and Al. The lower curve is the structure predicted to be stable at that relative atomic volume (i.e., pressure). At relative atomic volume = 1 (the right edge of each plot), we see that the computations correctly predict the crystal structures for the case of no applied pressure at 0 K (i.e., α-Sm for Na, HCP for Mg, and FCC for Al). Only 1 GPa of pressure is needed to reach the transformation point (compression to about 0.8 of original atomic volume), where Na's α-Sm structure shifts to BCC. In the Mg case, the transformation from HCP to BCC is predicted to occur at about 0.6, which corresponds to a pressure of 57 GPa. In Al, a transformation from FCC to BCC is predicted for about 0.35, which occurs at 130 GPa.

Predictions of transition metals' crystal structures are difficult due to the role of the *d* electrons in bonding, the large number of interactions that must be considered, and the magnetic effects in the first row of the transition metals. Figure 1.12 shows the results from computations performed without accounting for magnetic effects for the 3*d* transition metals. Note that the equilibrium crystal structures predicted at ambient pressure ($\Omega/\Omega_0 = 1.0$) are correct for the nonmagnetic metals Sc, Ti, V, and Cu. The predictions for Cr and Ni are also correct, even though they have magnetic behavior that should be considered for best accuracy. The prediction for Mn is HCP (like its congeners, Tc and Re); the complex α-Mn structure (cI58) was not among the cases calculated. The prediction for Co is FCC, although the energy calculated for the true equilibrium phase (HCP) is nearly as low. The calculations for Fe predict a closest-packed structure; Fe's BCC structure at room temperature is a consequence of its ferromagnetism.

Similar computations generate some fascinating predictions that await experimental confirmation. For example, the group 10 metals Ni, Pd, and Pt are predicted to have their *sp* band move through the Fermi energy as pressure increases, eventually creating a bandgap that would make these metals semiconducting at sufficiently high pressure. This is a difficult prediction to verify experimentally in diamond-anvil cells, which are poorly suited to resistivity measurements.

1.6 PERIODIC TRENDS IN MATERIAL PROPERTIES

The periodicity of atoms electronic structures powerfully influences properties such as density (Fig. 1.13), electronegativity (Fig. 1.14), melting point, elastic modulus, compressibility, and coefficient of thermal expansion. In the alkali metals of group 1, the single outer *s* electron is the only participant in bonding, resulting in weak, low-melting crystal structures. The comparatively large spacings between the atoms give the alkali metals the lowest densities and the lowest electronegativities of all metallic elements. The alkaline earth metals (group 2) hybridize to provide one *s* and one *p* outer bonding electron. This additional bonding electron makes them substantially denser and more electronegative than the alkali metals, but these are still among the lightest and most reactive of metals (Table 11.1).

As progressively larger numbers of *d* electrons become available to participate in bonding, the transition metals of groups 3 to 8 display ever stronger bonding, and the shorter interatomic spacings that result from this stronger bonding raise densities. Maximum density is reached in the middle of each row of transition metals. Densities begin to decline before the *d* subshell approaches its maximum of 10 electrons, because it is the number of *unpaired d* electrons, not total *d* electrons, that determines how many can participate in bonding. In W, the ground-state electron structure is (Xe core) + $4f^{14}5d^46s^2$; however, the additional energy needed to promote a 6*s* electron to the 6*p* subshell is only 8 kcal/mol, so each W atom contributes

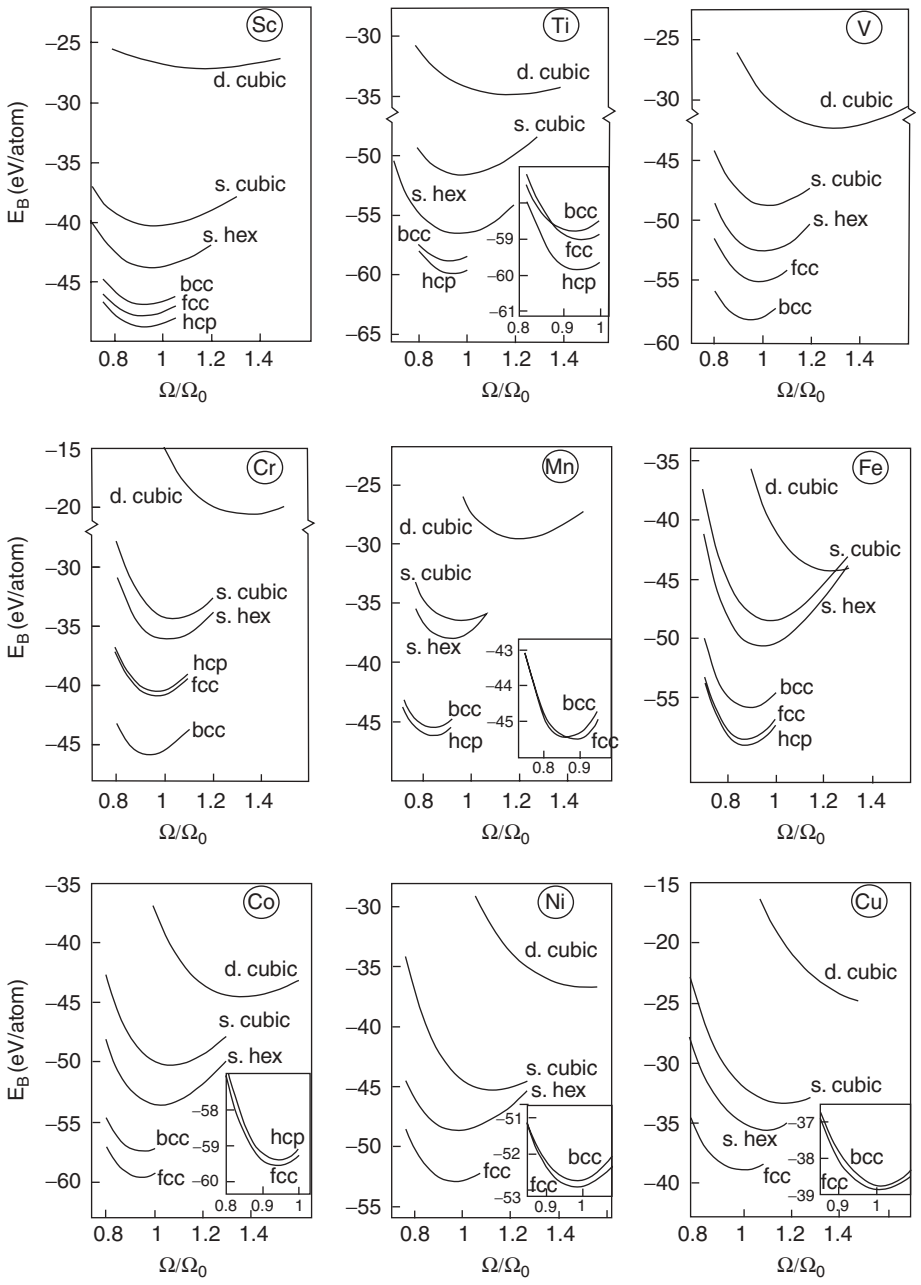

Fig. 1.12 Relative bonding energies of 3*d* transition metals at 0 K calculated for various crystal structures, not accounting for magnetic effects. The Ω/Ω_0 ratio is actual atomic volume/equilibrium atomic volume ($\Omega/\Omega_0 = 1$ at ambient pressure). (Redrawn from Paxton et al., 1992.)

six electrons for bonding rather than four. As a result, W is the highest-melting and one of the densest metallic elements. As the *d* subshell fills in groups 9 to 11, the total number of unpaired electrons available for bonding decreases, and the metals become lower melting and less dense.